Available online at www.scholarsresearchlibrary.com

Scholars Research Library

Der Pharmacia Lettre, 2016, 8 (18):167-179
(http://scholarsresearchlibrary.com/archive.html)

ISSN 0975-5071
USA CODEN: DPLEB4

A Thermodynamical and Electrochemical Investigation of Quinoxaline Derivatives as Corrosion Inhibitors for Mild Steel in 1 M Hydrochloric Acid Solution

H. Lgaz[1,2], M. Saadouni[3], R. Salghi[2*], S. Jodeh[4], Y. Ramli[5], A. Souizi[3] and H. Oudda[1]

[1]*Laboratory of separation methods, Faculty of Science, University Ibn Tofail PO Box 242, Kenitra, Morocco*
[2]*Laboratory of Applied Chemistry and Environment, ENSA, Université Ibn Zohr,PO Box 1136, 80000 Agadir, Morocco*
[3]*Laboratory of Organic, Organometallic and Theoretical Chemistry, Faculty of Science, Ibn Tofaïl University, 14000 Kenitra, Morocco*
[4]*Department of Chemistry, An-Najah National University, P. O. Box 7, Nablus, Palestine*
[5]*Laboratory of Medicinal Chemistry – Medical and Pharmaceutical College University Mohammed V of Rabat, Morocco*

ABSTRACT

The influence of four quinoxaline derivatives (QNs) namely, (E)-1-benzyl-3-(4-methoxystyryl)quinoxalin-2(1H)-one (QN1), (E)-3-(2-(furan-2-yl)vinyl)quinoxalin-2(1H)-one (QN2), (E)-3-(4-methoxystyryl)quinoxalin-2(1H)-one (QN3), and (E)-3-styrylquinoxalin-2(1H)-one (QN4) on the mild steel corrosion in 1 M HCl was studied by weight loss and electrochemical methods. Results showed that QN1 shows maximum inhibition efficiency of 93% at 5×10^{-3} M concentration. Polarization study revealed that the QNs act as mixed type inhibitors. EIS measurements showed that the studied compounds inhibit mild steel corrosion by adsorbing on the steel surface. Results showed that inhibition efficiency increases with concentration and decreases with the rises of the temperature from 303 to 333K. Adsorption of QNs on the mild steel surface obeyed the Langmuir adsorption isotherm.

Keywords: Mild steel, Corrosion, HCl, Quinoxaline derivatives, EIS, Polarization, Thermodynamic study.

INTRODUCTION

Despite the liability of mild steel for corrosion, acid solution is frequently used during several industries and industrial processes including chemical processing, petroleum production, acid pickling, acid cleaning, ore production, oil well acidification and acid descaling[1–6] due to its high corrosion resistance and inexpensive properties[7–14]. The use of organic inhibitors draws much attention due to their high efficiency, ease of synthesis, and cost-effective nature in order to protect the metal from corrosion in aggressive acid solution[11–19]. Generally, organic inhibitors inhibit metallic corrosion by adsorbing on the surface and thereby forming a protective barrier between metal and electrolyte (1 M HCl)[20–23]. The adsorption of these inhibitors on metallic surface are influenced by several factors such as molecular size of inhibitor, nature of substituents, nature of metal and electrolyte[24–28]. Organic compounds containing heteroatoms including nitrogen, sulfur, and/or oxygen with polar functional groups and conjugated double bonds have been reported as effective corrosion inhibitor[29–32].

Quinoxaline derivatives are important class of organic compounds with nitrogen heteroatoms and aromatic rings. Majority of these compounds are non-toxic, biodegradable, and possess wide biological activities. They have been widely used as dyes, pharmaceutics and photochemical materials. Their industrial importance in relation to their ability to inhibit metal corrosion has also been reported[33–36].

In view of this, four synthesized quinoxaline namely (E)-1-benzyl-3-(4-methoxystyryl)quinoxalin-2(1H)-one (**QN1**), (E)-3-(2-(furan-2-yl)vinyl)quinoxalin-2(1H)-one (**QN2**), (E)-3-(4-methoxystyryl)quinoxalin-2(1H)-one (**QN3**), and (E)-3-styrylquinoxalin-2(1H)-one (**QN4**) were synthesized to study mild steel corrosion inhibition in 1 M HCl using weight loss, electrochemical impedance spectroscopy (EIS) and potentiodynamic polarization. The effect of temperature on the inhibited acid–metal reaction is highly complex because many changes occur on the metal surface, such as rapid etching and desorption of the inhibitor and the inhibitor itself, in some cases, may undergo decomposition and/or rearrangement[37]. In this case, it very important to calculate some thermodynamic functions for additional insights about the inhibition and/or the adsorption processes which can help us to determine the type of adsorption of the studied inhibitors.

MATERIALS AND METHODS

Materials

The steel used in this study is a mild steel (Euronorm: C35E carbon steel and US specification: SAE 1035) with a chemical composition (in wt%) of 0.370 % C, 0.230 % Si, 0.680 % Mn, 0.016 % S, 0.077 % Cr, 0.011 % Ti, 0.059 % Ni, 0.009 % Co, 0.160 % Cu and the remainder iron (Fe). The mild steel samples were pre-treated prior to the experiments by grinding with emery paper SiC (120, 600 and 1200); rinsed with distilled water, degreased in acetone in an ultrasonic bath immersion for 5 min, washed again with bidistilled water and then dried at room temperature before use.

Solutions

The aggressive solutions of 1.0 M HCl was prepared by dilution of analytical grade 37% HCl with distilled water. The concentration range of quinoxaline derivatives used was 1×10^{-4}M to 5×10^{-3} M.

Corrosion tests

Weight loss

Gravimetric measurements were carried out at definite time interval of 6 h at room temperature using an analytical balance (precision ± 0.1 mg). The mild steel specimens used have a rectangular form (length = 2 cm, width = 2 cm, thickness = 0.08 cm). Gravimetric experiments were carried out in a double glass cell equipped with a thermostated cooling condenser containing 80 mL of test solution. After immersion period, the steel specimens were withdrawn, carefully rinsed with bidistilled water, ultrasonic cleaning in acetone, dried at room temperature and then weighed.

Electrochemical impedance spectroscopy

The electrochemical measurements were carried out using Volta lab (Tacussel- Radiometer PGZ 100) potentiostate and controlled by Tacussel corrosion analysis software model (Volta master 4) at under static condition. The corrosion cell used had three electrodes. The reference electrode was a saturated calomel electrode (SCE). A platinum electrode was used as auxiliary electrode of surface area of 1 cm^2. The working electrode was mild steel. All potentials given in this study were referred to this reference electrode. The working electrode was immersed in test solution for 30 minutes to a establish steady state open circuit potential (E_{ocp}). After measuring the E_{ocp}, the electrochemical measurements were performed. All electrochemical tests have been performed at 303 K. The EIS experiments were conducted in the frequency range with high limit of 100 kHz and different low limit 10 mHz at open circuit potential, with 10 points per decade, at the rest potential, after 30 min of acid immersion, by applying 10 mV ac voltage peak-to-peak. Nyquist plots were made from these experiments.

Potentiodynamic polarization

The electrochemical behaviour of mild steel sample in inhibited and uninhibited solution was studied by recording anodic and cathodic potentiodynamic polarization curves. Measurements were performed in the 1.0 M HCl solution containing different concentrations of the tested inhibitors by changing the electrode potential automatically from -800 to -200 mV versus corrosion potential at a scan rate of 2 $mV.s^{-1}$. The linear Tafel segments of anodic and cathodic curves were extrapolated to corrosion potential to obtain corrosion current densities (I_{corr}).

Inhibitors

The present investigation was undertaken to examine the corrosion inhibition capacity of quinoxaline derivatives in 1.0 M HCl solution on mild steel and their stability at the temperature range of 303 to 333 K using potentiodynamic polarisation curves (PDP), weight loss and electrochemical impedance spectroscopy (EIS) methods. The adsorption isotherm of inhibitor on steel surface was determined. Kinetic parameters are calculated and discussed in detail. Figure 1 shows the molecular structure of the quinoxaline derivatives utilised in this investigation.

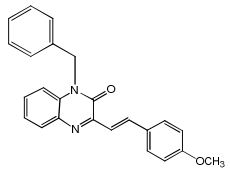

(E)-1-benzyl-3-(4-methoxystyryl)quinoxalin-2(1H)-one (QN1)

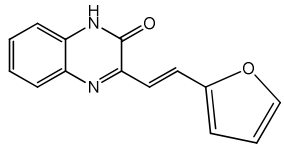

(E)-3-(2-(furan-2-yl)vinyl)quinoxalin-2(1H)-one (QN2)

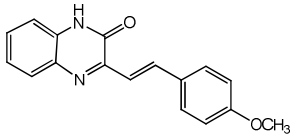

(E)-3-(4-methoxystyryl)quinoxalin-2(1H)-one (QN3)

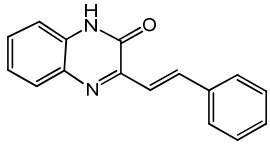

(E)-3-styrylquinoxalin-2(1H)-one (QN4)

Figure 1: Chemicals structures of quinoxaline derivatives

RESULTS AND DISCUSSION

Effect of concentration inhibitor

Weight loss

Variation of the inhibition efficiency (η%), corrosion rate (C_R) and surface coverage (θ) obtained from weight loss measurements at different concentrations of the studied QNs at 303 K are given in Table 1. The corrosion rate, C_R (mg/cm^2×h), surface coverage (θ) and inhibition efficiency η_w (%) of each concentration were calculated using the following equations[1]:

$$W = \frac{\Delta m}{St} \quad (1)$$

$$\eta_W = \left(\frac{W_{uninh} - W_{inh}}{W_{uninh}} \right) \times 100 \quad (2)$$

Where Δm is the average weight loss (mg), S is the surface area of specimens (cm^2), and t is the immersion time (h), W_{uninh} and W_{inh} are corrosion rates in the absence and presence of inhibitor, respectively.

Table 1. Effect of QNs concentrations on corrosion data of mild steel in 1.0 M HCl

Inhibitor	Concentration (mol/L)	W (mg/cm^2 × h)	E_W (%)
HCl	1	1.135	-
	$\mathbf{5 \times 10^{-3}}$	0.079	**93**
QN1	$\mathbf{1 \times 10^{-3}}$	0.147	87
	$\mathbf{5 \times 10^{-4}}$	0.215	81
	$\mathbf{1 \times 10^{-4}}$	0.283	75
	$\mathbf{5 \times 10^{-3}}$	0.113	**90**
QN2	$\mathbf{1 \times 10^{-3}}$	0.158	86
	$\mathbf{5 \times 10^{-4}}$	0.238	79
	$\mathbf{1 \times 10^{-4}}$	0.329	71
	$\mathbf{5 \times 10^{-3}}$	0.136	**88**
QN3	$\mathbf{1 \times 10^{-3}}$	0.215	81
	$\mathbf{5 \times 10^{-4}}$	0.295	74
	$\mathbf{1 \times 10^{-4}}$	0.340	70
	$\mathbf{5 \times 10^{-3}}$	0.147	**87**
QN4	$\mathbf{1 \times 10^{-3}}$	0.249	78
	$\mathbf{5 \times 10^{-4}}$	0.329	71
	$\mathbf{1 \times 10^{-4}}$	0.374	67

Results showed that the η% increases with increasing concentration and maximum inhibition efficiency was obtained at 5×10^{-3} M concentration. The observed order of η% for all studied compounds is:

QN1 (93%) > QN2 (90%) > QN3 (88%) > QN4 (87%)

Electrochemical impedance spectroscopy

The Nyquist plots in the absence and presence of different studied concentrations of the QNs are shown in Figure 2. Nyquist plots give one semicircle in the absence and presence of different concentrations of QNs suggesting that inhibition of metallic corrosion taking place in the present study is due to retardation of electron charge transfer process[10]. Deviation from the perfect semicircle is generally attributed to the frequency dispersion as well as to the inhomogeneities of the surface and mass transport resistant[16]. Examination of the Figure 2 shows that in the presence of QNs the diameter of the Nyquist plots increases with increasing concentration. The increased diameter of the Nyquist plots in the presence of QNs suggested that values of charged transfer resistance (R_{ct}) increase due to formation of protective film[11,14]. The electrochemical parameters, including R_{ct}, Q and n, obtained from fitting the recorded EIS data using the electrical circuit of Figure 3 are listed in Table 2. The impedance of the CPE isexpressed as follows[17].

$$Z_{CPE} = \frac{1}{Q(j\omega)^n} \tag{3}$$

Where Q is the CPE constant, n is the phase shift which can be explained as a degree of surface inhomogeneity, j is the imaginary unit and ω is the angular frequency. Depending on the values of n, CPE can represent resistance (n=0), capacitance (n=1), inductance (n= -1) and Warburg impedance (n=0.5). The values of the interfacial capacitance C_{dl} can be calculated from CPE parameter values Q and n using the expression[30]:

$$C_{\mathrm{dl}} = \left(Q\times R^{1-n}\right)^{1/n} \tag{4}$$

The R_{ct} values were used to calculate the inhibition efficiency, η_{EIS}(%), (listed in Table 2), using the following equation:

$$\eta_{\mathrm{EIS}}\% = \frac{R_{ct}^{i} - R_{ct}^{\circ}}{R_{ct}^{i}}\times 100 \tag{5}$$

Where R_{ct}° and R_{ct}^{i} are the charge transfer resistance in absence and in presence of inhibitor, respectively.

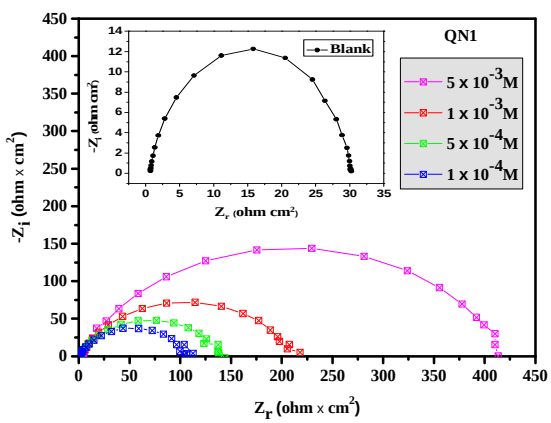

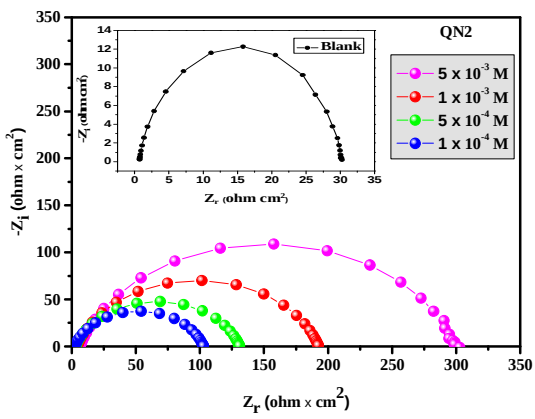

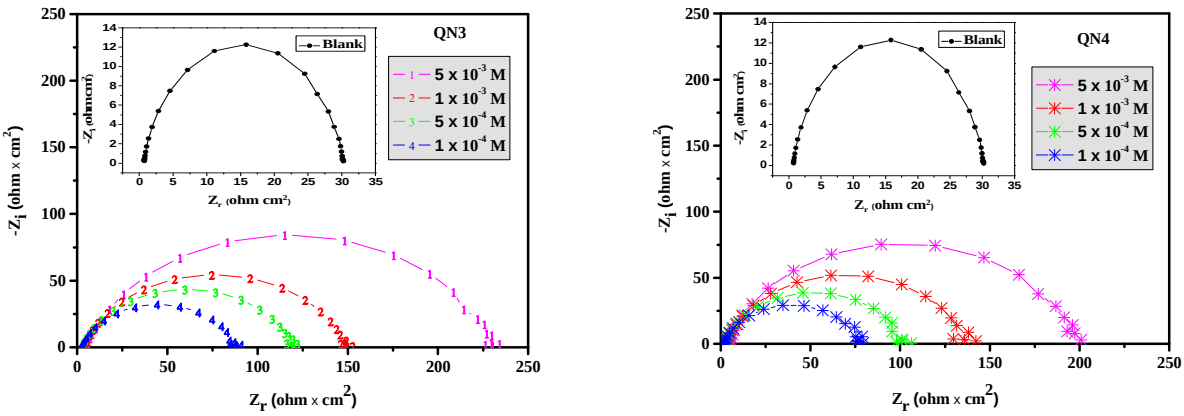

Figure 2: Nyquist diagrams of mild steel with different concentrations of QNs at 303K

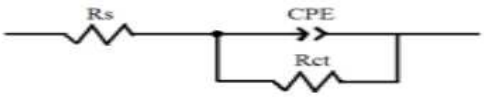

Figure 3: Equivalent electrical circuit model

Inspection of the Table 2 reveals that values of R_{ct} increase with increasing QNs concentration suggesting that extent of surface coverage and η% increases with inhibitor concentration. The increased values of R_{ct} and decreased values of C_{dl} in the presence of QNs are attributed either due to decrease in local dielectric constant or an increase in the thickness of electrical double layer or due to combined effect of both which is resulted due to adsorption of QNs at metal/electrolyte interfaces[5,7,11].

Table 2. Electrochemical impedance parameters for corrosion of mild steel in acid medium at various contents of QNs at 303 K

Inhibitor	Concentration (M)	R_{ct} $(\Omega \times cm^2)$	n	$Q \times 10^{-4}$ $(S^n\Omega^{-1}cm^{-2})$	C_{dl} $(\mu F/cm^2)$	E_{EIS} (%)	θ
Blank	1.0	29.35	0.89	1.7610	91.86	-	-
	5×10^{-3}	419.28	0.87	0.2596	13.21	**93**	0.93
QN1	1×10^{-3}	209.64	0.86	0.3993	18.33	86	0.86
	5×10^{-4}	139.76	0.85	0.7129	31.61	79	0.79
	1×10^{-4}	108.7	0.84	1.0676	45.68	73	0.73
	5×10^{-3}	293.5	0.81	0.4378	15.76	**90**	0.90
QN2	1×10^{-3}	183.43	0.82	0.5498	20.04	84	0.84
	5×10^{-4}	127.6	0.8	0.9978	33.51	77	0.77
	1×10^{-4}	97.83	0.83	1.1878	47.69	70	0.70
	5×10^{-3}	225.76	0.8	0.6588	23.01	**87**	0.87
QN3	1×10^{-3}	146.75	0.81	0.7578	26.37	80	0.80
	5×10^{-4}	117.4	0.79	1.1378	36.12	75	0.75
	1×10^{-4}	81.53	0.82	1.3478	50.07	64	0.64
	5×10^{-3}	195.67	0.84	0.6602	28.83	**85**	0.85
QN4	1×10^{-3}	133.41	0.83	0.8178	32.41	78	0.78
	5×10^{-4}	101.21	0.8	1.2108	40.28	71	0.71
	1×10^{-4}	73.37	0.84	1.3618	56.63	60	0.60

Polarization curves

Potentiodynamic polarization studies were carried out in absence and presence of different concentrations of the investigated inhibitors in order to understand the process of anodic oxidative metallic dissolution and cathodic reductive hydrogen evolution. The potentiodynamic polarization curves for mild steel in absence and presence inhibitors are shown in Figure 4. The values of potentiodynamic polarization parameters such as corrosion potential (E_{corr}), corrosion current density (i_{corr}), cathodic Tafel slope (β_c) were obtained from the polarization curves through

extrapolation method and are included in Table 3. The i_{corr} values were used to calculate the inhibition efficiency, η_{PDP}(%), (listed in Table 3), using the following equation[16]:

$$\eta_{PDP}\% = \frac{I_{corr} - I_{corr(i)}}{I_{corr}} \times 100 \qquad (6)$$

Where, I_{corr} and $I_{corr(i)}$ are the corrosion current density in absence and presence of inhibitor, respectively.

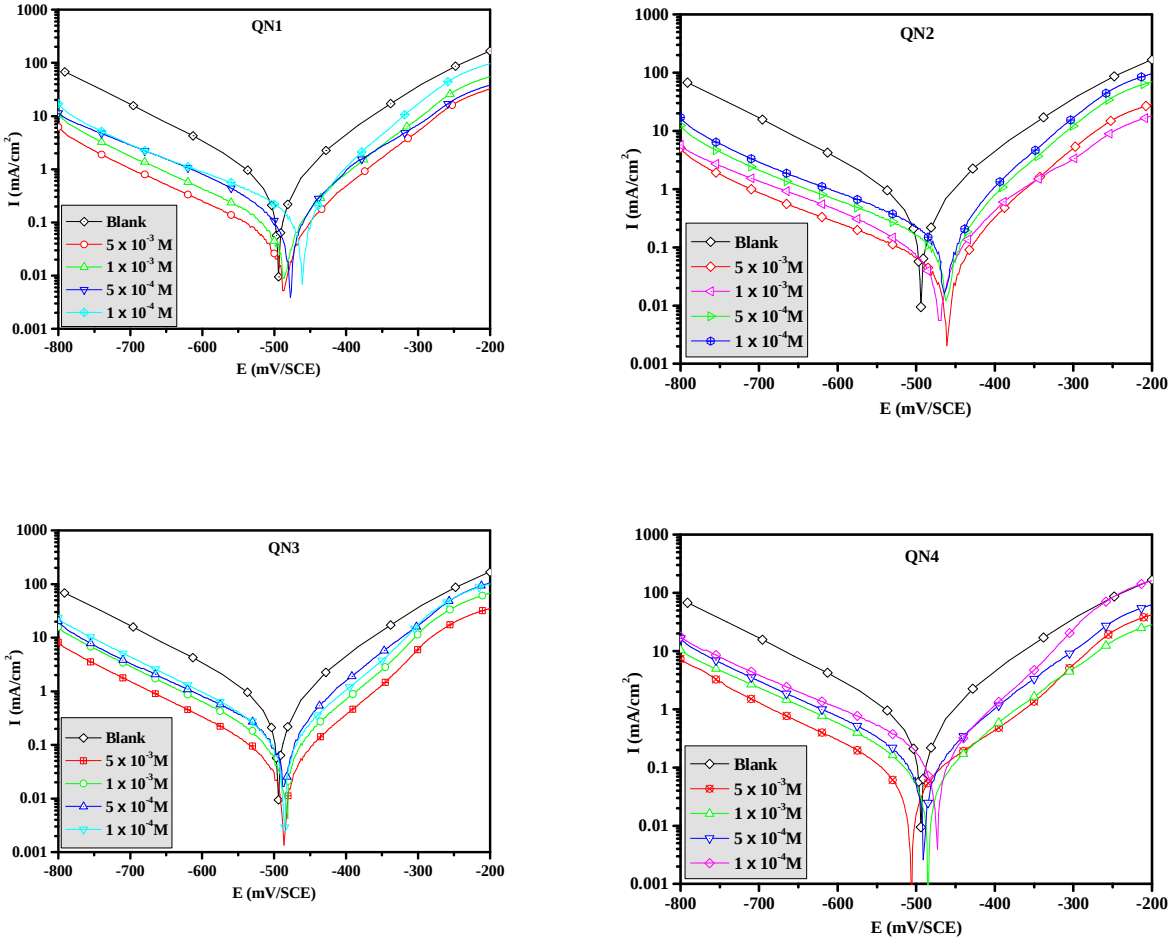

Figure 4. Potentiodynamic polarization curves of mild steel in 1.0 M HCl in the presence of different concentrations of QNs at 303 K

It can be seen from the results (Table 3 and Figure 4) that presence of QNs significantly reduced the values of corrosion current densities for both anodic and cathodic half reactions. This finding indicates that inhibitors undertaken in the present study successfully inhibited both anodic oxidative dissolution of mild steel and cathodic reductive evolution of hydrogen[38]. The decreased values of i_{corr} in presence of inhibitors are attributed due to blocking of the active centers present on the metallic surface[39]. It is obvious from the Figure 4 that any significant change in E_{corr} values observed in presence of inhibitors, indicating that investigated inhibitors act as mixed type inhibitors[40].

Table 3. Electrochemical parameters of mild steel at various concentrations of QNs in 1.0 M HCl and corresponding inhibition efficiency

Inhibitor	Concentration (M)	$-E_{corr}$ (mV/SCE)	$-\beta_c$ (mV dec^{-1})	i_{corr} (µA cm^{-2})	E_{PDP} (%)	Θ
HCl	1.0	496	150.19	564	-	-
QN1	5×10^{-3}	487	159	45.12	**92**	0.92
	1×10^{-3}	486	160	73.32	87	0.87
	5×10^{-4}	479	154	107.16	81	0.81
	1×10^{-4}	465	195	124.08	78	0.78
QN2	5×10^{-3}	463	193	50.76	**91**	0.91
	1×10^{-3}	470	201	90.24	84	0.84
	5×10^{-4}	462	197	112.8	80	0.80
	1×10^{-4}	465	196	129.72	77	0.77
QN3	5×10^{-3}	488	152	62.04	**89**	0.89
	1×10^{-3}	483	150	95.88	83	0.83
	5×10^{-4}	485	158	135.36	76	0.76
	1×10^{-4}	487	151	152.28	73	0.73
QN4	5×10^{-3}	508	156	78.96	**86**	0.86
	1×10^{-3}	486	166	112.8	80	0.80
	5×10^{-4}	490	167	146.64	74	0.74
	1×10^{-4}	476	176	174.84	69	0.69

Effect of temperature and activation parameters

The variation of inhibition efficiency from PDP measurements in the absence and presence of optimum concentrations of the QNs at several studied temperatures is shown in Figure 5 (For QN1) and Table 4. Results showed that inhibition efficiency for all studied QNs decreases on increasing solution temperature which can be attributed to the quick desorption of adsorbed inhibitor molecules from the surface in addition to the decomposition of these molecules at elevated temperatures[41].

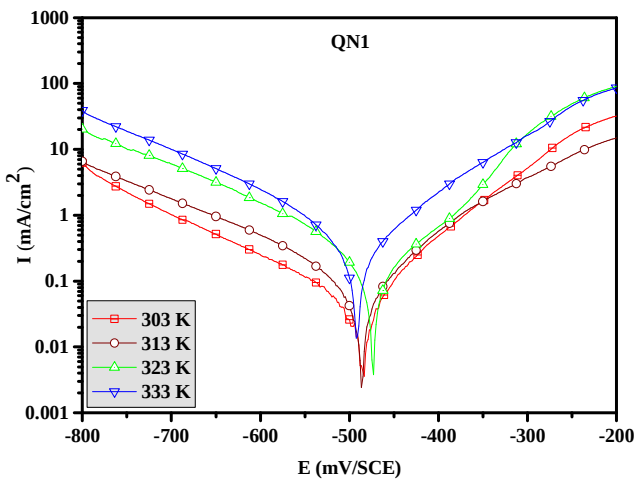

Figure 5. Potentiodynamic polarization curves of mild steel in 1 M HCl in the presence 5×10^{-3} M of QN1 at different temperatures

The significance of the temperature on mild steel dissolution in 1 M HCl in the absence and presence of QNs can be best represented by Arrhenius equation[41]:

$$i_{corr} = k\exp\left(-\frac{E_a}{RT}\right) \quad (7)$$

Where E_a is the apparent activation corrosion energy, R is the universal gas constant and k is the Arrhenius pre-exponential constant.

Arrhenius plots for the corrosion density of carbon steel in the case of QNs are given in Figure 6. Values of apparent activation energy of corrosion (E_a) for mild steel in 1 M HCl with the absence and presence of QNs were determined from the slope of $Ln(I_{corr})$ versus 1/T plots and shown in Table 5. It is noticeable that the values of *E*a are higher for inhibited acid solution than that for uninhibited solution. This implies that, in the presence of the QNs the rate of mild steel dissolution is decreased due to the adsorption of QNs on mild steel and more energy barrier is achieved[5,17,41,42].

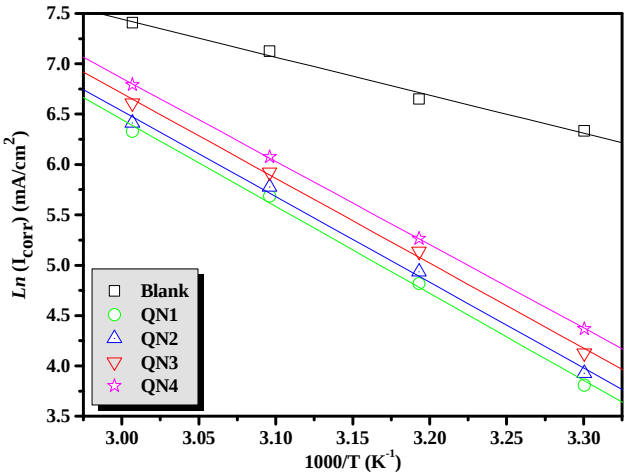

Figure 6. Arrhenius plots of carbon steel in 1 M HCl with and without 5×10^{-3} M of QNs

Table 4. Various corrosion parameters for mild steel in 1 M HCl in absence and presence of optimum concentration of QNs at different temperatures

Temperature (K)	Inhibiteur	E_{corr} (mV/SCE)	I_{corr} (µA/cm^2)	E_I (%)	θ
	HCl		564	-	-
	QN1	487	45.12	92	0.92
303	QN2	463	50.76	91	0.91
	QN3	488	62.04	89	0.89
	QN4	508	78.96	86	0.86
	HCl		773	-	-
	QN1	489	123.68	84	0.84
313	QN2	472	139.14	82	0.82
	QN3	495	170.06	78	0.78
	QN4	492	193.25	75	0.75
	HCl		1244	-	-
	QN1	476	311.0	75	0.75
323	QN2	480	323.0	74	0.74
	QN3	493	373.2	70	0.70
	QN4	494	435.4	65	0.65
	HCl		1650	-	-
	QN1	494	561.0	66	0.66
333	QN2	480	610.0	63	0.63
	QN3	497	742.5	55	0.55
	QN4	487	891.0	46	0.46

Activation parameters like enthalpy (ΔH_a) and entropy (ΔS_a) for the dissolution of carbon steel in 1 M HCl in the absence and presence of 5×10^{-3} M **QNs** were calculated from the transition state equation:

$$i_{corr} = \frac{RT}{Nh}\exp\left(\frac{\Delta S_a}{R}\right)\exp\left(-\frac{\Delta H_a}{RT}\right) \quad (8)$$

Where *h* is Planck's constant, *N* is the Avogadro number, *R* is the universal gas constant, ΔH_a is the enthalpy of activation and ΔS_a is the entropy of activation.

Figure 7 shows that the Arrhenius plots of $Ln(i_{corr}/T)$ versus 1/T gave straight lines with slope ($-\Delta H_a/R$) and intercept (Ln R/Nh + $\Delta S_a/R$) from where ΔH_a and ΔS_a values were calculated. The activation parameters are given in Table 5.

Table 5. The values of activation parameters for carbon steel in 1 M HCl in the absence and presence of 5×10^{-3}M of QNs

Inhibitors	R^2	A (mA/cm^2)	Ea (kJ mol^{-1})	ΔHa (kJ mol^{-1})	ΔSa (kJ mol^{-1}K^{-1})	Ea-ΔHa
Blank	0.995	1.224×10^{8}	31.01	28.36	-98.85	2.65
QN1	0.997	7.891×10^{13}	70.88	68.22	12.32	2.66
QN2	0.998	5.814×10^{13}	69.79	67.15	9.83	2.64
QN3	0.998	5.574×10^{13}	69.19	66.55	9.48	2.64
QN4	0.999	4.011×10^{13}	67.85	65.21	6.74	2.64

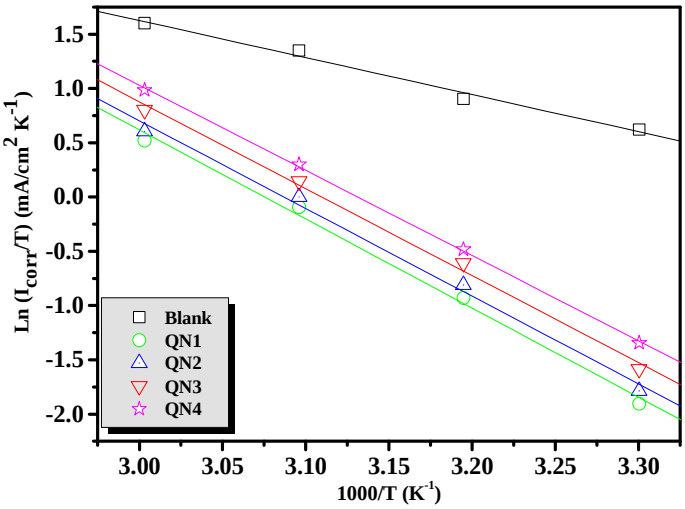

Figure 7. Arrhenius plots of mild steel in 1 M HCl with and without 5×10^{-3} M of QNs

The positive sign of the endothermic enthalpy reflects the nature of the dissolution of the steel. We note that the variation of the activation energy E_a and the enthalpy of ΔH_a vary in the same way with the concentration of inhibitor, which satisfies the relationship between E_a and thermodynamics as ΔH_a: $E_a - \Delta H_a = RT$. The entropy of activation, Δ Sa, in the absence of the inhibitor is negative, implying that the rate-determining step for the activated complex is the association rather than the dissociation step, while in the presence of the inhibitor, Δ Sa is positive, which implies that the adsorption process is accompanied by an increase in entropy, which is the driving force for the adsorption of inhibitor onto the carbon steel surface[43].

Adsorption isotherm and standard adsorption free energy

Generally, organic compounds inhibit corrosion by adsorbing on the metallic surfaces. The adsorption of inhibitors on the metal surfaces may be chemisorption, physisorption or physiochemisorption. A typical adsorption process involves the replacement of the adsorbed water molecule (H_2O_{ads}) by inhibitor molecules present in aqueous solution (Org_{aq}) at metal/electrolyte interface as represented below[41]:

$$Org_{aq} + xH_2O_{ads} \leftrightarrow Org_{ads} + xH_2O_{aq}$$

where *x* is the number of water molecules replaced by one molecule of organic inhibitors. An attempt was made to plot the values of surface coverage (θ) derived from *PDP* experiment against different QNs concentrations in order to obtained the best adsorption isotherm. However, if we assume that the adsorption of our inhibitors adsorption isotherm follows Langmuir, the rate of surface coverage (θ) for different concentrations in acidic medium is evaluated by the method of weight loss according to the report E_{PDP} (%) / 100 and using the following equation[42]:

$$\frac{C_{inh}}{\theta} = \frac{1}{K_{ads}} + C_{inh} \quad (9)$$

Where C_{inh} is the concentration of inhibitor and K_{ads} the adsorptive equilibrium constant.

Figure 8 shows the curves of the variation of C_{inh} / θ according to the concentration C_{inh} for the quinoxalines compounds. The linearity of these curves indicates that the adsorption of our inhibitors on the surface of mild steel in 1 M HCl, is according to the Langmuir isotherm model. The validity of this approach is confirmed by the strong correlation (R^2= 0.999).

The values of K_{ads} obtained from the reciprocal of intercept of Langmuir isotherm line are listed in Table 6, together with the values of the Gibbs free energy of adsorption ΔG°_{ads} calculated from the equation:

$$K_{ads} = (\frac{1}{55.5})\exp(-\frac{\Delta G^{\circ}_{ads}}{RT}) \quad (10)$$

Where R is gas constant and T is absolute temperature of experiment and the constant value of 55.5 is the concentration of water in solution.

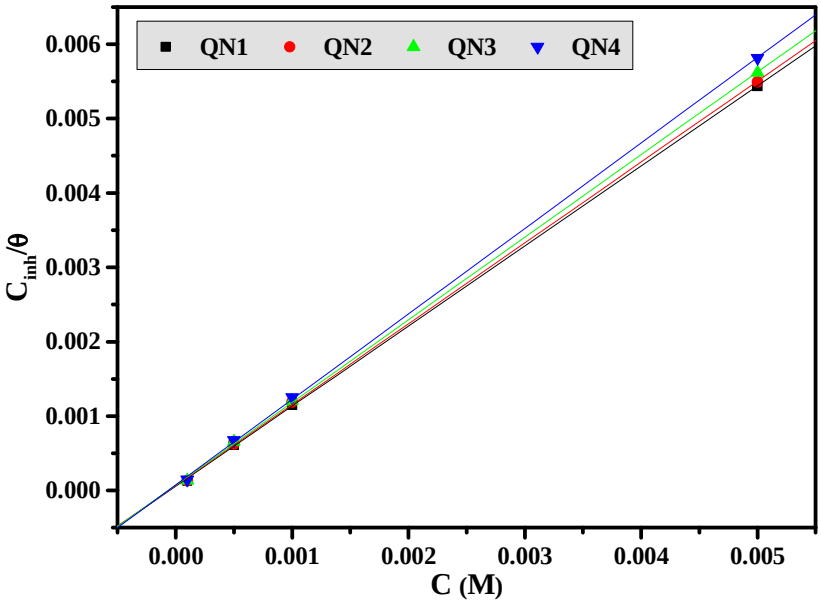

Figure 8. Adsorption isotherm according to Langmuir's model derived from *PDP* measurement

Table 6. Thermodynamic parameters for the adsorption of QNs in 1 M HCl on the carbon steel at 303 K

Inhibiteurs	Coefficient de régression linéaire	K_{ads} (L/mol)	ΔG_{ads} (kJ/mol)
QN1	0.99994	18114	-34.8
QN2	0.99990	15193	-34.3
QN3	0.99991	13866	-34.1
QN4	0.99992	13328	-34.0

The high values of adsorption equilibrium constants K_{ads} correspondent's quinoxaline compounds to reflect the high adsorption capacity of these inhibitors on the surface of mild steel in acidic 1 M HCl. This suggests that this inhibitor can best recoveries, where it's most effective protection against corrosion.

The negative values of the standard free energy of adsorption indicates a spontaneous adsorption of molecules on the surface of our mild steel and also the strong interaction between the inhibitors molecules and the metal surface[44]. Literature study reveals that the value of ΔG_{ads} up to −20 kJ/mol or less negative is related to the electrostatic interactions between inhibitor and metallic surfaces (physisorption), while the value of ΔG_{ads} is around −40 kJ/mol

or more negative related to the charge sharing between inhibitor and metallic surfaces (chemisorption)[44]. However, in our present case the values of ΔG_{ads} range in between −34. 8 and −34.0 kJ/mol suggesting that adsorption of the QNs on mild steel surface follows physiochemisorption (mixed mode of adsorption)[16,25,44].

Mechanism of inhibition

It has been established that the inhibitor molecule containing heteroatoms particularly nitrogen, sulfur, oxygen and phosphorus inhibits metallic corrosion in acid solution by adsorbing at the metal/electrolyte interfaces. Previously, it has been investigated by several authors[34,45,46] that heteroatoms of the inhibitor molecule in acid solution easily undergo protonation due to the presence of unshared electron pair on these atoms, and therefore in acid solution organic compounds exist in cationic form. On the other hand the metallic surface becomes negatively charged due to the presence of uniform layer counter ion (chloride ions of hydrochloric acid) present over the metallic surface[34,45,46]. These appositively charged species attracted each other through electrostatic force of attraction, and therefore it can be concluded that first step involves physisorption during the QNs adsorption processes [34,45,46]. However, as soon as QNs comes in its neutral form by release of hydrogen gas at cathode, the chemisorption takes place by transfer of free unshared electron pairs of heteroatoms into empty d-orbitals of surface iron atoms [46]. Moreover, this type of electron transfer causes excessive accumulation of negative charge on electron rich metallic surface which renders it to transfer its electrons to the empty anti-bonding molecular orbitals of the inhibitor through retro-donation. Both donation and retro-donation strengthen adsorption of the QNs molecules on mild steel surface through synergism[34,46]. The pictorial presentation of the interaction responsible for adsorption of QNs on mild steel surface is shown in Figure 9.

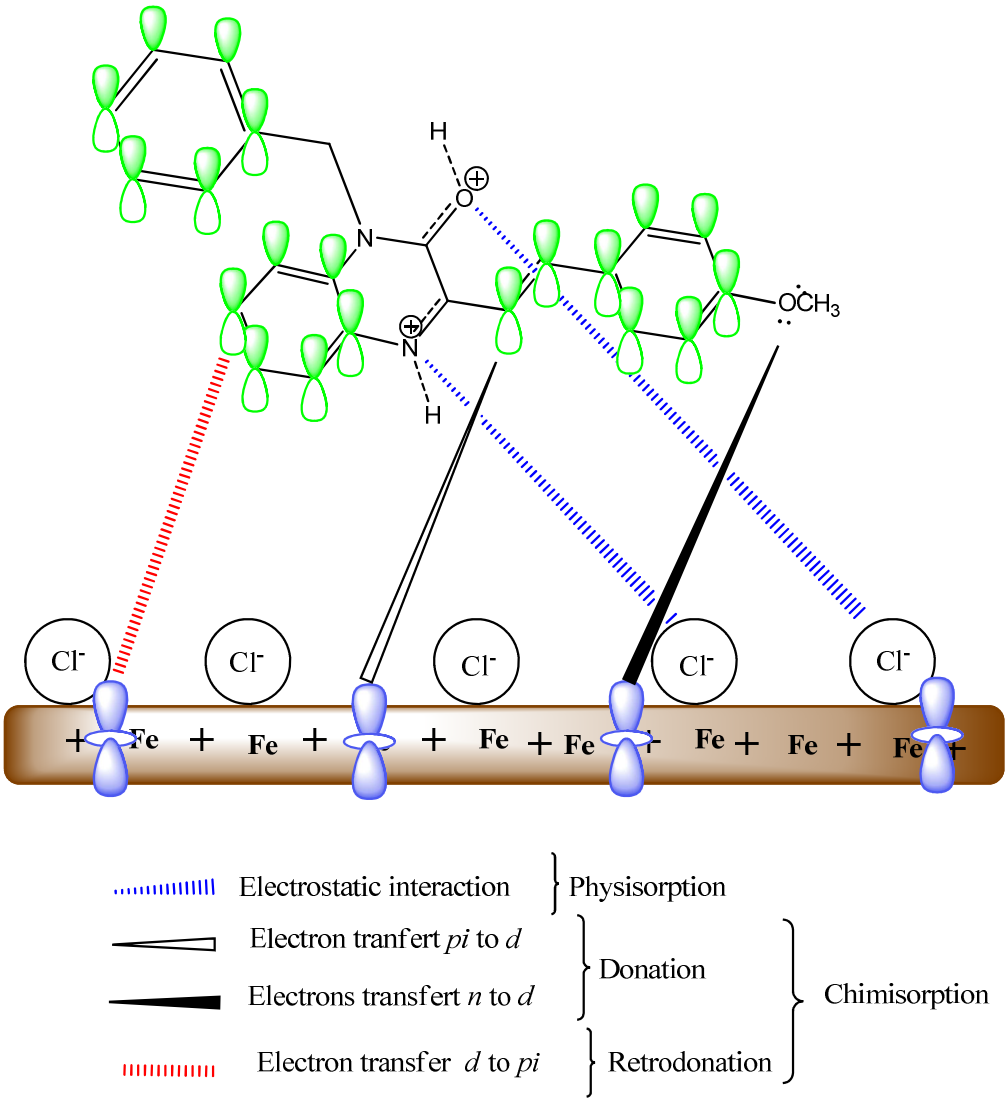

Figure 9: Pictorial presentation of adsorption of QN1 on mild steel surface in acid solution

CONCLUSION

Quinoxaline derivatives have been studied as corrosion inhibitors for mild steel in 1 M HCl solution and the following conclusions were arrived at:

1) QN1, QN2, QN3 and QN4 inhibit the corrosion of mild steel in 1 M HCl solution and the inhibition efficiency increases with increase in concentration of the inhibitors.
2) Both polarization and impedance electrochemical techniques showed that the studied compounds are mixed type inhibitors and the order of inhibition efficiency at 5×10^{-3} M is:

QN1 > QN2 > QN3 > QN4.

3) The inhibitors adsorb spontaneously on mild steel surface and their adsorption behavior obeys Langmuir adsorption isotherm.
4) Different mechanisms of adsorption and inhibition are possible and have been proposed.

REFERENCES

[1] B El Makrini, H Lgaz, K Toumiat, R Salghi, S Jodeh, G Hanbali, M Belkhaouda, and M Zougagh, *Res. J. Pharm. Biol. Chem. Sci.* **2016**, 7, 2277.
[2] M Larouj, H Lgaz, H Serrar, H Zarrok, H Bourazmi, A Zarrouk, A Elmidaoui, A Guenbour, S Boukhris, and H Oudda, *J. Mater. Environ. Sci.* **2015**, 6, 3251.
[3] L Adardour, H Lgaz, R Salghi, M Larouj, S Jodeh, M Zougagh, O Hamed, and H Oudda, *Pharm. Lett.* **2016**, 8, 212.
[4] H Lgaz, A Anejjar, R Salghi, S Jodeh, M Zougagh, I Warad, M Larouj, and P Sims, *Int. J. Corros. Scale Inhib.* **2016**, 5, 209.
[5] M Saadouni, M Larouj, R Salghi, H Lgaz, S Jodeh, M Zougagh, and A Souizi, *Pharm. Lett*. **2016**, 8, 65.
[6] H Lgaz, S Rachid, M Larouj, M Elfaydy, S Jodeh, H Abbout, B Lakhrissi, K Toumiat, and H Oudda, *Moroc. J. Chem.* Mor. **2016**, 4, 592.
[7] L Adardour, H Lgaz, R Salghi, M Larouj, S Jodeh, M Zougagh, O Hamed, and M Taleb, *Pharm. Lett*. **2016**, 8, 173.
[8] L Adardour, H Lgaz, R Salghi, M Larouj, S Jodeh, M Zougagh, I Warad, and H Oudda, *Pharm. Lett.* **2016**, 8, 126.
[9] H Lgaz, R Salghi, and S Jodeh, *Int. J. Corros. Scale Inhib*. **2016**, 5, 347.
[10] H Lgaz, M Larouj, M Belkhaouda, R Salghi, S Jodeh, I Warad, H Oudda, and A Chetouani, *Moroc. J. Chem.* **2016**, 4, 101.
[11] B El Makrini, K Toumiat, H Lgaz, R Salghi, S Jodeh, G Hanbali, M Belkhaouda, and M Zougagh, *Res. J. Pharm. Biol. Chem. Sci*. **2016**, 7, 2286.
[12] L Adardour, M Larouj, H Lgaz, M Belkhaouda, R Salghi, S Jodeh, A Salman, H Oudda, and M Taleb, *Pharma Chem*. **2016**, 8, 152.
[13] N Lotfi, H Lgaz, M Belkhaouda, M Larouj, R Salghi, S Jodeh, H Oudda, and B Hammouti, *Arab. J. Chem. Environ. Res.* **2015**, 1, 13.
[14] M Larouj, H Lgaz, S Rachid, S Jodeh, M Messali, M Zougagh, H Oudda, and A Chetouni, *Moroc. J. Chem*. **2016**, 4, 567.
[15] L Afia, M Larouj, H Lgaz, R Salghi, S Jodeh, S Samhan, and M Zougagh, *Pharma Chem*. **2016**, 8, 22.
[16] K Toumiat, Y El Aoufir, H Lgaz, R Salghi, S Jodeh, M Zougagh, and H Oudda, *Res. J. Pharm. Biol. Chem. Sci.* **2016**, 7, 1210.
[17] M Saadouni, M Larouj, R Salghi, H Lgaz, S Jodeh, M Zougagh, and A Souizi, *Pharm. Lett.* **2016**, 8, 96.
[18] L Afia, M Larouj, R Salghi, S Jodeh, M Zougagh, A Rasem Hasan, and H Lgaz, *Pharma Chem*. **2016**, 8, 166.
[19] B El Makrini, M Larouj, H Lgaz, R Salghi, A Salman, M Belkhaouda, S Jodeh, M Zougagh, and H Oudda, *Pharma Chem*. **2016**, 8, 227.
[20] M Larouj, M Belkhaouda, H Lgaz, R Salghi, S Jodeh, S Samhan, H Serrar, S Boukhris, M Zougagh, and H Oudda, *Pharma Chem*. **2016**, 8, 114.
[21] M Larouj, H Lgaz, S Rachid, H Oudda, S Jodeh, and A Chetouani, *Moroc. J. Chem*. 2016, 4, 425.
[22] Y El Aoufir, H Lgaz, K Toumiat, R Salghi, S Jodeh, M Zougagh, A Guenbour, and H Oudda, *Res. J. Pharm. Biol. Chem. Sci*. **2016**, 7, 1200.
[23] M Elfaydy, H Lgaz, R Salghi, M Larouj, S Jodeh, M Rbaa, H Oudda, K Toumiat, and B Lakhrissi, *J. Mater. Environ. Sci*. **2016**, 7, 3193.
[24] K Toumiat, Y El Aoufir, H Lgaz, R Salghi, S Jodeh, M Zougagh, and H Oudda, *Res. J. Pharm. Biol. Chem. Sci*. **2016**, 7, 1209.

[25] Y El Aoufir, H Lgaz, K Toumiat, R Salghi, S Jodeh, M Zougagh, A Guenbour, and H Oudda, *Res. J. Pharm. Biol. Chem. Sci*. **2016**, 7, 1219.
[26] A Bousskri, R Salghi, A Anejjar, S Jodeh, M A Quraishi, M Larouj, H Lgaz, M Messali, S Samhan, and M Zougagh, *Pharma Chem.* **2016**, 8, 67.
[27] H Lgaz, O Benali, R Salghi, S Jodeh, M Larouj, O Hamed, M Messali, S Samhan, M Zougagh, and H Oudda, *Pharma Chem*. **2016**, 8, 172.
[28] H Lgaz, Y ELaoufir, Y Ramli, M Larouj, H Zarrok, R Salghi, A Zarrouk, A Elmidaoui, A Guenbour, EM Essassi, and H Oudda, *Pharma Chem.* **2015**, 7, 36.
[29] O Krim, S Jodeh, M Messali, B Hammouti, A Elidrissi, K Khaled, R Salghi, and H Lgaz, *Port. Electrochimica Acta* **2016**, 34, 213.
[30] M J Reddy, C Verma, EE Ebenso, KK Singh, MA Quraishi, *Int J Electrochem Sci*, **2014**, 9, 4884–4899
[31] B El Makrini, H Lgaz, M Larouj, R Salghi, A Rasem Hasan, M Belkhaouda, S Jodeh, M Zougagh, and H Oudda, *Pharma Chem*. **2016**, 8, 256.
[32] H Lgaz, R Salghi, S Jodeh, Y Ramli, M Larouj, K Toumiat, MA Quraishi, H Oudda, and W Jodeh, *J. Steel Struct. Constr.* **2016**, 2, 1.
[33] S Singh, J Singh, M Ingle, R Mishra, P V Khadikar, M M Heravi, K Bakhtiari, M H Tehrani, N M Javadi, and H A Oskooie, **2006**.
[34] I Obot and N Obi-Egbedi, *Mater. Chem. Phys.* **2010**, 122, 325.
[35] S Dailey, W J Feast, R J Peace, I C Sage, S Till, and E L Wood, *J. Mater. Chem.* **2001**, 11, 2238.
[36] A Gazit, H App, G McMahon, J Chen, A Levitzki, and F D Bohmer, *J. Med. Chem.* **1996**, 39, 2170 ().
[37] F Bentiss, M Lebrini, and M Lagrenée, *Corros. Sci*. **2005**, 47, 2915.
[38] D K Singh, S Kumar, G Udayabhanu, and R P John, *J. Mol. Liq*. **2016**, 216, 738.
[39] A A Farag, A S Ismail, and M A Migahed, *J. Mol. Liq*. **2015**, 211, 915.
[40] K K Anupama, K Ramya, and A Joseph, *J. Mol. Liq*. **2016**, 216, 146.
[41] C Verma, M A Quraishi, and A Singh, *J. Mol. Liq*. **2015**, 212, 804.
[42] C Verma, E E Ebenso, I Bahadur, I B Obot, and M A Quraishi, *J. Mol. Liq.* **2015**, 212, 209.
[43] X Li, S Deng, H Fu, and G Mu, *Corros. Sci*. **2008**, 50, 2635.
[44] C Verma, M A Quraishi, E E Ebenso, I B Obot, and A El Assyry, *J. Mol. Liq*. **2016**, 219, 647.
[45] D K Yadav, B Maiti, and M Quraishi, *Corros. Sci*. **2010**, 52, 3586.
[46] S Deng, X Li, and X Xie, *Corros. Sci*. **2014**, 80, 276.